WOOD DENSITY AND ANATOMICAL PROPERTIES IN SUPPRESSED-GROWTH TREES: COMPARISON OF TWO METHODS

*David W. Vahey**

Materials Research Engineer

J. Y. Zhu†

Research General Engineer, Scientific Team Leader

and

C. Tim Scott

General Engineer
USDA Forest Service, Forest Products Laboratory
One Gifford Pinchot Drive
Madison, WI 53726–2398

(Received June 2006)

ABSTRACT

Interest in the commercial value of small-diameter timber has led to testing core samples with SilviScan to characterize density and transverse fiber dimensions. Data showed that latewood density and tracheid diameter in suppressed-growth material can vary spatially on a scale comparable to the 50-μm resolution of the instrument used in our testing. An optical imaging method called Ring Profiler was developed to determine what effect SilviScan's resolution had on the measurements. A single suppressed-growth specimen of Douglas-fir was used to develop the method. Ring Profiler measurements of the specimen showed that SilviScan overestimated latewood tracheid radial diameters by 59% in growth rings averaging 200-μm width. In those same growth rings, SilviScan latewood density was found to be 19% too low. In all growth rings measured by Ring Profiler, latewood wall thicknesses were anisotropic. Radial and tangential values averaged 13% less than the isotropic wall thickness calculated from SilviScan data. Ring Profiler density measurement from binarized images of wood cross-sections was found to correlate well with SilviScan X-ray density (r-squared = 0.907); however, better images and an objective method for thresholding are needed for accuracy over a large sample space. With these improvements and automated scanning of samples, Ring Profiler could be an attractive, inexpensive complement to SilviScan.

Keywords: SilviScan, tracheid, density, diameter, wall thickness, anisotropy, image analysis, resolution, suppressed growth, small diameter, thinnings, pulp.

INTRODUCTION

On National Forest lands in the western United States, restoring forest health through selective thinning produces a very large number of small-diameter trees, many of which exhibit suppressed growth. To offset the high cost of thinning operations, it is desirable to find high value, large volume uses for these trees. One viable approach is to use them as a source of fiber for making paper. Forest thinnings have not readily been accepted as a reliable fiber source by our partners in the pulp and paper industry of the Pacific Northwest. The industry lacks a fundamental understanding of the basic material properties of thinnings, which can be very different from those of traditional pulp-

* Corresponding author: dvahey@fs.fed.us
† Member of SWST

© 2007 by the Society of Wood Science and Technology

wood. To encourage the industry to use small-diameter trees, it is necessary to demonstrate that the fibers obtained from these trees have desirable characteristics that make them amenable to paper production. A goal of our research is to relate the wood anatomical properties of suppressed-growth trees to the optimized manufacture of thermomechanical pulp made from such trees (Klungness et al. 2006).

The morphology of wood fibers, in particular the dimensions of tracheid wall thickness and lumen diameter, directly influences fiber mechanical properties. These in turn affect the processing and properties of both lumber and paper (Seth 1990; Kibblewhite and Bawden 1991; Skinnarland et al. 1995; Seth et al. 1997). Because fiber morphology is dictated by wood anatomical properties (Evans et al. 1997; Evans et al. 1999; Jones and Corson 1996; Kang et al. 2004; Jang et al. 2005; Zhu et al. 2007), the understanding and characterization of these properties in forest thinnings allow us to predict the value of these materials relative to conventional pulpwood.

Near infrared (NIR) spectroscopy has been developed to characterize wood anatomical properties (Schimleck and Evans 2004; Schimleck et al. 2004). However, NIR technique relies on multivariate calibration and requires an established anatomical database specific for each tree species of interest. Diversity of forest thinning materials makes a useful database difficult to obtain. Optical microscopy and the scanning electron microscope (SEM) have been widely used for wood anatomical characterization through direct visualization (Jang et al. 2005; DeGroot and Kuster 1986; Reme and Helle 2002; Ivkovich et al. 2002; Liu et al. 2002; Midorikawa et al. 2005). SilviScan (CSIRO Forestry and Forest Products, Australia), a commercial instrument that combines optical microscopy and X-ray densitometry, has been widely used for anatomical characterization of trees in fast-growing plantations (Evans et al. 1997; Evans et al. 1999). Whereas SilviScan analysis is capable of quickly measuring a sample with good statistical significance, the limited spatial resolution of 50 μm in our testing (25 μm in new instruments) coupled with line-of-sight measurements through curved growth rings makes it unsuitable for measurements of suppressed-growth trees with annual ring widths less than several hundred microns. This may lead to incorrect values of morphological properties in the radial direction. For example, one tree experienced suppressed-growth conditions resulting in an annual growth ring of 160-μm width, containing only 8 fiber layers in the radial direction. The latewood growth layer containing two or three fibers (20 μm radially) is small compared to the 50-μm resolution of SilviScan. This leads to individual density measurements based on X-rays that sampled both earlywood and latewood fibers. The resulting density profile points to a high degree of uniformity between earlywood and latewood that may not exist. In addition, the SilviScan approach of calculating an isotropic wall thickness from measured density and diameter may not work well for the latewood tracheids of suppressed-growth trees. These can be irregular in shape and much thicker in the tangential direction than in the radial direction.

SilviScan was used to analyze wood anatomical properties of samples from Klungness et al. (2006). The results indicated that a suppressed-growth environment produced tracheids with greater uniformity between earlywood and latewood in terms of tracheid wall thickness compared to trees growing under normal conditions. According to Rudie et al. (1994), greater uniformity between earlywood and latewood could result in less cutting and damaging of fibers in thermomechanical pulping. Therefore, the SilviScan analysis of Klungness et al. (2006) could have a significant effect on the valuation and utilization of forest thinning materials and deserves confirmation through more accurate measurements.

The present research involves the development of an optical imaging technique to do this. The technique was developed with reference to a single Douglas-fir (*Pseudotsuga menziesii*) sample, one that shows both suppressed and normal growth over different parts of its lifetime. The work is similar to that of Reme and Helle

(2002), who used SEM images and sophisticated signal processing to characterize two trees in detail. Our characterization offers less detail but simpler signal processing that may be more amenable to rapid, automated measurement.

For ease of presentation, we refer to our image-based counterpart to SilviScan as Ring Profiler. Ring Profiler replaces the X-ray density component of SilviScan with image analysis. It also performs the imaging tasks of SilviScan at higher magnification. The disadvantages of Ring Profiler are that its density measurement is indirect and it lacks the capability to measure the microfibril angle, an important feature of SilviScan for solid-wood applications. The main advantages of Ring Profiler are that it is readily implemented and it has the ability to directly measure radial and tangential tracheid wall thickness.

EXPERIMENTAL METHODS

Sample

A 70-year core from a Douglas-fir tree was selected for development of Ring Profiler and its comparison with SilviScan. This core was selected because its growth rings were greater than 1 mm from age 10 to 30, and under 1 mm from 30 to 70, with one exception. We considered ages 10 to 47 to represent "normal growth" and ages 48 to 70 to represent "suppressed growth." The average growth-ring widths for these periods were 1.33 mm for normal growth and 0.24 mm for suppressed growth. The largest suppressed-growth ring width was 0.45 mm. The methods of sample preparation and measurement for SilviScan testing are documented by Evans (1994). The core's dimensions were 65 mm (radial) by 7 mm (longitudinal) by 2 mm (tangential). Ring Profiler analysis was applied to the core as received following SilviScan testing.

Imaging

Figure 1 shows a schematic of the experimental arrangement. White light from an EG&G Xenon source (Perkin-Elmer Optoelectronics, Fremont, CA) was transmitted over fiber optics to two 25-mm-long by 2-mm-wide Fostec light lines (Schott North America, Elmsford, NY). These were butted against the 7-mm longitudinal side of the core about 4 mm below the viewing surface. Some of the light entering the sample is captured by the fiber walls and diffuses along the length of the fibers to the viewing surface (Palviainen and Silvennoinen 2001). Most of this light is red or near infrared. Light captured in the lumen tends not to be confined because of the absence of total-internal reflection. Light from the lumen that does approach the viewing surface is absorbed by wood dust from the polishing phase of sample preparation. As a result, there is good contrast between fiber-wall material and lumen, with the fiber-wall material showing as light and the lumen showing as dark. A 20× microscope objective captures the light emitted at the viewing surface and images it on a standard RS170 black-and-white Hitachi KP-M1 CCD (Hitachi, Ltd. Tokyo, Japan) camera with 640 by 480 resolution. The useful field of view is 300 μm (radial) by 233 μm (tangential).

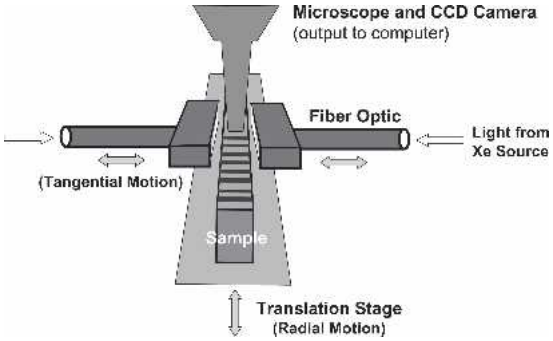

FIG. 1. Schematic diagram of Ring Profiler optical arrangement.

Between images, the core is moved in the radial growth direction using a stage manually driven with a screw having a pitch of 1.57/mm (40/inch). Each annual growth ring is measured, beginning with the one nearest the bark and continuing to the ninth ring from the pith, where the amount of light becomes insufficient for a good image. (Two rings in between were inadvertently skipped.) In annual rings wider than 300 μm, an image was made with the last latewood

at the right edge of the field of view. A second image was then made with the first earlywood at the left edge of the field of view. Annual ring widths were determined from the known pitch of the screw that translates the sample. These were in good agreement with the ring widths determined by SilviScan and reported here. In the tangential growth direction, the camera images captured about one-eighth of the 2-mm sample width, generally the center portion. Flexibility to move one field in either direction to find a good image was useful, since ray cells and other nontracheid wood material occasionally complicated the image processing.

Images were saved in the JPEG (.jpg) format and processed with Optimas software (Media Cybernetics, Silver Spring, Maryland), version 5.23. Typical file size was 15 kb. The first processing was local smoothing to reduce the influence of lighting nonuniformity on the measurements. A region of interest (ROI) was selected that always included the first earlywood or the last latewood, and extended to include as much as possible of earlywood or latewood that had the same general tracheid size and wall thickness. Typical regions of interest were 125 μm radial by 233 μm tangential (for latewood) and 200 μm radial by 233 μm tangential (for earlywood). For suppressed-growth material, regions of interest were compressed as necessary to avoid the mixing of earlywood and latewood in the analysis. The smallest radial ROI for suppressed growth was 37 μm. For comparison with Ring Profiler results, we selected single SilviScan measurements, usually corresponding to the least or greatest SilviScan density values for a given growth ring. Since we selected single measurements, the window represented by the selected SilviScan data was 50 μm.

Ring Profiler's pixel resolution of about 0.6 μm is sufficient for direct measurement of average wall thickness for a group of fibers representing earlywood or latewood within a growth ring, an advantage over SilviScan. The tradeoff is in the field of view. The rectangular cores measured by SilviScan are about 2 mm in the tangential growth direction. Our image spans only about 12% of this width. To cover the entire area of a core section 60-mm radial by 2-mm tangential, 1,600 images would be required. By restricting images to the first earlywood and the last latewood from each growing season, about 100 images provide a reasonable optical counterpart to SilviScan measurements for an entire core. This approach offers the flexibility to measure only latewood or only earlywood at any one time. Since SilviScan is automated, it will always have occasions where the 50-μm measurement window includes both earlywood and latewood.

Measurements

Tracheid diameter and thickness—Method I (Line scan).—The various methods of Ring Profiler measurement are suggested by Fig. 2. A rectangle is used to highlight a ROI identifying either the first earlywood or (as in Fig. 2) the last latewood of a growing season. The radial and tangential size of the ROI is known from calibration. Several lines are drawn within the ROI that cut across the walls of adjacent tracheids. These lines are used in the measurement of tracheid double-wall thickness by Method I. Software extracts a profile of luminance values along the lines. A profile of moving-average luminance values is also generated. The number of adjacent pixels averaged is about the number

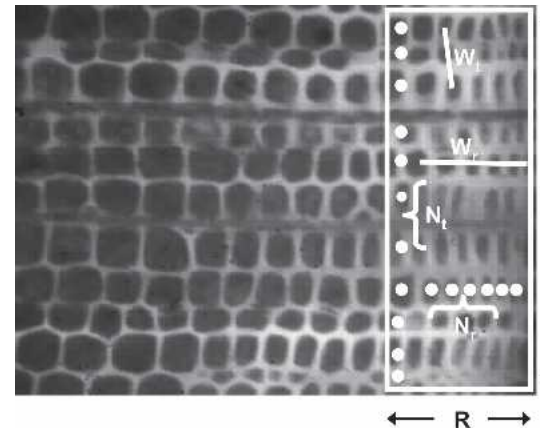

FIG. 2. Schematic indication of graphics procedures for calculating tracheid diameters and wall thicknesses in the radial (R) and tangential (T) directions.

spanned by a typical double-wall thickness. If the actual profile luminance value at a point of interest exceeds that of the moving average, the point is taken to represent tracheid wall material rather than lumen. In this way, a binarized profile is established to determine the width of the double walls. Although the precision of the measurement for any one double wall is limited, the average over a number of them can be quite accurate. Typically, we process five profiles, each of which crosses three double walls, for a total of 15 measurements in a ROI. For very narrow growth rings, we are limited to as few as five measurements. Lines are either radial or tangential to capture the different thickness in each direction. Using this Method I, detailed wall-thickness measurements were made of tracheids for 17 of the core's 70 growth rings.

Method I can easily be generalized to measure tracheid diameter as well as wall thickness. (Note the use of the word "diameter" to describe the cross-sectional extent of non-circular tracheids. "Width" is limited to growth rings, and "thickness" is limited to tracheid wall material to avoid confusion). It is convenient to draw new lines through tracheids encompassing one double-wall thickness and the adjacent lumen and measure their lengths directly using software. This approach was used on seven selected growth rings with 10 diameter measurements averaged for each ROI.

Tracheid diameter—Method II (Counting).—Figure 2 indicates another approach to diameter measurement that is in good agreement with Method I. A vertical line of dots identifies the number of rows of tracheids, N_t, filling the length T of the ROI in the tangential direction. The average tangential diameter of the tracheids is the ratio T/N_t. Similarly, the average radial diameter of the tracheids is the ratio R/N_r. The best estimates of N_t and N_r will be fractions rather than integers. The selected approach was to estimate N_t (because tangential uniformity is better than radial uniformity), count the total number of fibers in the ROI, and then divide by N_t to determine N_r. This approach gives very similar results for average tracheid diameter to that of Method I. It has the advantages of involving all the tracheids in the calculation and of being simple enough to apply to all growth rings rather than to a selected few.

Wood density.—Ring Profiler density was determined by thresholding the gray-level image in the ROI to convert it to a binary image. Contributions from ray cells were minimized by selecting images without ray cells, when possible. Ring Profiler density consists of the fractional area coverage of tracheid wall material times its nominal density, 1.5 g/cm^3 (Reme and Helle 2002; Kellogg and Wangaard 1969). The software provides the fractional area coverage, making this an easy measurement to implement. The difficulty comes in determining the appropriate threshold to avoid labeling part of the lumen as wall material and vice versa.

Using the higher-resolution capabilities of Ring Profiler to measure tracheid diameter, wall thickness, and density allows us to evaluate the strengths and weaknesses of SilviScan for characterizing suppressed-growth material. Table 1

TABLE 1. *Comparison of SilviScan and Ring Profiler.*

Measurement features	Method	
	SilviScan	Ring Profiler
Density	Direct, X-ray transmission	Indirect, percentage of image area covered by cellulosic material
Microfibril angle	Direct, X-ray diffraction	Not available
Tracheid diameters	Direct, image line metrology	Direct, image line metrology or counting tracheids in region of interest
Tracheid wall thickness	Indirect, calculation	Direct, image line metrology
Field of view	100% sample coverage in 2-mm by 50-μm steps	3% sample coverage overall, in 300-μm by 233-μm steps
Earlywood/Latewood separation	Uncontrolled	Controlled
Optical resolution	2.6 μm/pixel	0.6 μm/pixel

shows a comparison between SilviScan and Ring Profiler as demonstrated by the present work.

RESULTS

Tracheid diameter

Figure 3 shows the trend of earlywood and latewood radial tracheid diameter starting at 10 years, using SilviScan and Ring Profiler Methods I and II. There is better agreement in the case of earlywood than latewood. In the last 20 years before harvest, when ring widths average 220 μm, SilviScan latewood measurement includes an earlywood contribution. This produces values for latewood radial diameter that trend toward the larger values measured for earlywood. In the juvenile tree, rectangular ROIs superimposed on curved growth rings produce a similar averaging effect. Ring Profiler measurements avoid these problems by virtue of their higher resolution. Seven individual radial diameters measured by Method I (line scan) agree with the continuous results of Method II (counting). Both disagree with SilviScan results in the early and later years of the core's history.

Figure 4 shows relatively little difference between earlywood and latewood tangential diameter during years of suppressed growth. Spatial resolution limitations are therefore not detectable. Consistent with this, both SilviScan and Ring Profiler tangential diameter measurements agree during years of suppressed growth. During years of normal growth, SilviScan tangential diameters are higher than Ring Profiler diameters, typically by 25%. This discrepancy points to an

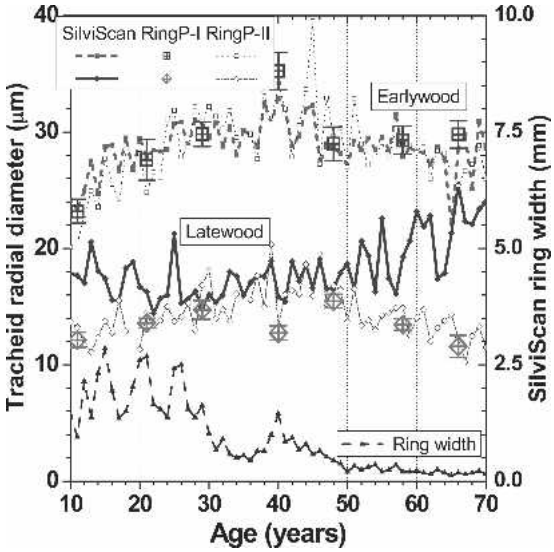

FIG. 3. Tracheid radial diameter of Douglas-fir earlywood and latewood, measured by SilviScan and Ring Profiler methods, including detailed (Method I) measurements for seven individual growth rings.

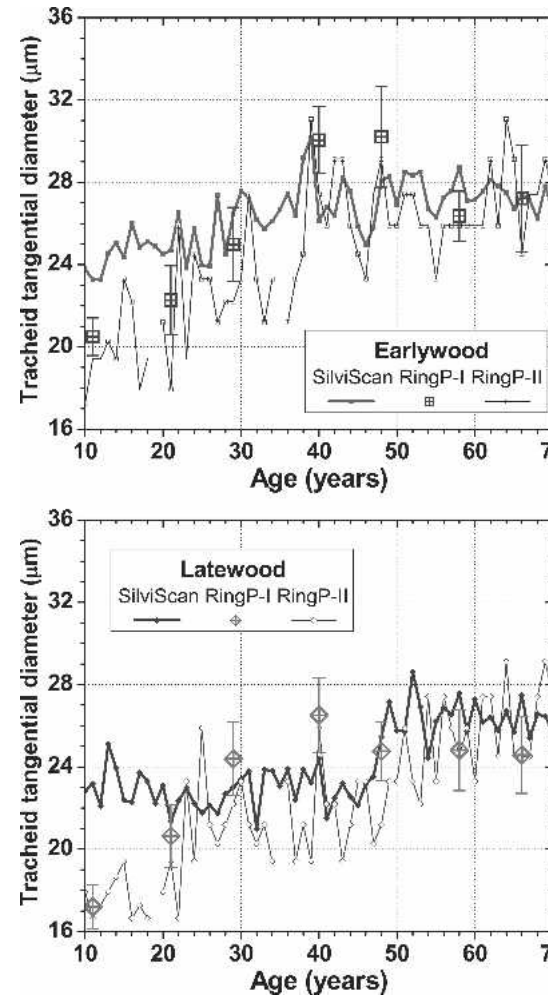

FIG. 4. Tracheid tangential diameter of earlywood (top) and latewood (bottom), measured by SilviScan and Ring Profiler methods, including detailed (Method I) measurements of seven individual growth rings.

error in one of the measurements, although it is not possible to say which one. Alternatively, the discrepancy could result from sampling different areas of the specimen, and not be directly attributable to either method.

Tracheid wall thickness

Ring Profiler Method I has the spatial resolution to measure both tangential and radial wall thickness. For the more variable case of latewood, tangential wall thickness exceeds radial wall thickness by about 60% in our specimen of Douglas-fir. SilviScan calculates an isotropic wall thickness from radial diameter, tangential diameter, and density. We can improve the calculation by incorporating the wall-thickness anisotropy determined by Ring Profiler. If w_R and w_T are the radial and tangential wall thicknesses, respectively, and if $\alpha = w_T/w_R$ is the anisotropy, then

$$w_T = \frac{R\alpha + T}{4} - \frac{1}{2}\sqrt{\frac{(R\alpha + T)^2}{4} - \frac{R\alpha TD}{d}} \quad (1)$$

where R is the radial diameter, T is the tangential diameter, D is the local bulk density, and d is the tracheid wall density, assumed to be 1.5 g/cm^3 (Reme and Helle 2002). When $\alpha = 1$ the formula reduces to that used by SilviScan to calculate the isotropic wall thickness, w (Evans 1994).

Figure 5 shows the resulting latewood wall thickness trend from applying SilviScan diameter and density data along with anisotropy data from the Ring Profiler measurements. During years of normal growth, calculated SilviScan wall thicknesses are higher than values measured by Ring Profiler. This reflects the larger diameter measurements by SilviScan in the normal-growth period, seen in both Figs. 3 and 4. In years of suppressed growth, the agreement between the calculated and measured wall thickness is good. This success may be interpreted in terms of cancellation of errors in the inputs to Eq. (1). Figure 3 shows that the SilviScan radial tracheid diameter during suppressed-growth years is overestimated. For the observed good agreement in Fig. 5 during these years, the

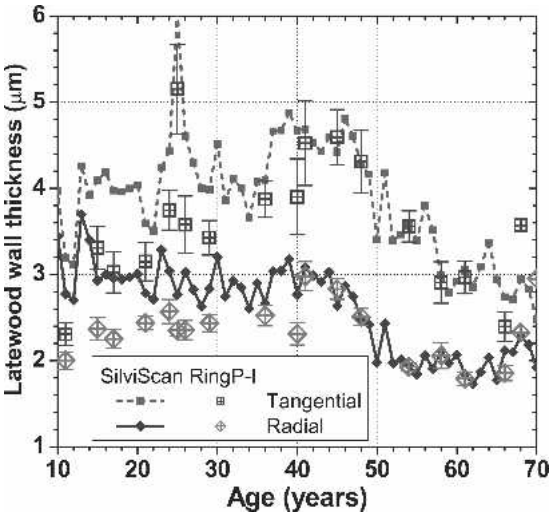

FIG. 5. Calculated tangential and radial wall thicknesses of latewood from SilviScan data using Ring Profiler anisotropies, along with actual Ring Profiler Method-I measurements for 17 individual growth rings.

X-ray density measurements of SilviScan must underestimate the true density. Both errors have their origin in the 50-μm spatial resolution of SilviScan, which limits its ability to resolve latewood density and diameter variations under suppressed-growth conditions. When the SilviScan results for density (too low) and diameter (too high) are inserted into Eq. (1), the errors tend to cancel. This qualitatively explains how the calculated SilviScan wall thickness can be in good agreement with that measured by Ring Profiler for suppressed-growth material.

Wood density

If we accept the validity of Ring Profiler measurements for wall thickness and tracheid diameter under suppressed-growth conditions, we can rearrange Eq. (1) to determine what bulk density, D, is consistent with the results. We then can compare this indirectly determined density with the directly measured SilviScan density to estimate the effects of spatial resolution.

The result of this analysis is shown in Fig. 6. Ring Profiler radial diameter is used in Eq. (1) in place of the SilviScan value for suppressed-growth rings corresponding to tree rings 48 to

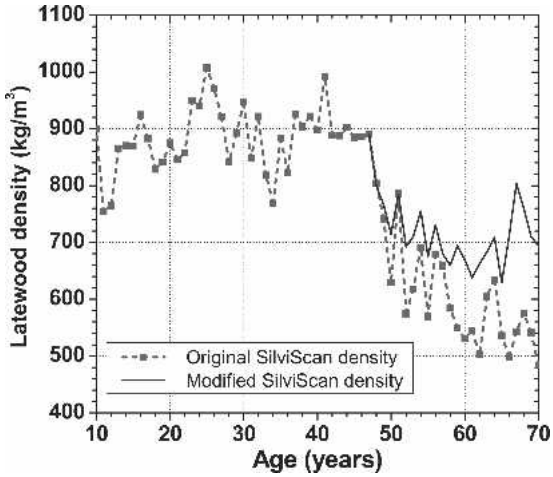

FIG. 6. Original SilviScan latewood density and modified density that results in correct wall thickness when Ring Profiler radial tracheid diameters are used in place of SilviScan radial diameters.

70. The largest ring width for these years is 450 μm and the average is 240 μm. The modified density shown in the graph combines with the Ring Profiler radial diameter, SilviScan's own tangential diameter, and Ring Profiler anisotropy to produce the SilviScan values for radial and tangential wall thickness shown in Fig. 5, which are in good agreement with the directly measured Ring Profiler values. The modified SilviScan density is higher than the reported SilviScan density for suppressed growth, though still less than the reported density for normal growth.

Another test of the usefulness of Ring Profiler is its ability to predict wood bulk density based on the percentage-area coverage by tracheid wall material. This calculation requires binarization of images like that of Fig. 2 to optimize the contrast between tracheid wall material (white) and lumen material (black). An estimate of the bulk density (excluding the influence of rays and other non-tracheid material) can be made by multiplying the percentage-area coverage by the nominal density of tracheid wall material, 1.5 g/cm^3 (Reme and Helle 2002; Kellogg and Wangaard 1969). When threshold levels for binarization were chosen subjectively, the linear fit with zero intercept predicted SilviScan density with an *R*-squared of 0.907, a slope of 1.08 and a standard error of 86.2 kg/m^3.

Upon reexamining the images corresponding to eight latewood test points from the correlation, we determined that the subjective choice of threshold was about 4% too high for optimal agreement between the SilviScan and Ring Profiler methods of density determination. Unfortunately, the method of sample preparation and illumination (Fig. 1) didn't produce latewood images with enough contrast between lumen and tracheid wall to produce histograms with bimodal structure. This would have facilitated means for objective threshold selection, for example, at the local minimum between the two modes.

CONCLUSIONS

The present work addressed the measurement of wood anatomical properties using a proven existing method, SilviScan (Evans 1994), and a complementary alternative called Ring Profiler. We conclude that Ring Profiler can have significant advantages over SilviScan for measuring trees with suppressed growth or anisotropic tracheid wall thickness. Although limited to a single Douglas-fir sample used to develop the method, the results are useful as a means for building hypotheses to test on larger numbers of samples from varied species when greater output from Ring Profiler becomes available (Reme and Helle 2002).

For growth rings narrower than 380 μm, we found a divergence between Ring-Profiler and SilviScan measurements of latewood radial tracheid diameter. SilviScan diameter values were larger and tended to approach the earlywood tracheid diameter as growth-ring widths decreased. This is consistent with the picture of a 50-μm resolution window that is broader than the latewood band being tested, and therefore forced to include some earlywood. The same picture suggests that measured density will tend to approach the lower-valued earlywood density, and we found this to be the case as well.

Another limitation of SilviScan measurements is that it computes an isotropic tracheid wall thickness (Evans 1994). We found that ear-

lywood wall thickness was essentially isotropic, but that latewood wall thickness was not. Anisotropic wall thickness has been measured for radiata pine, *Pinus radiata* (Cown 1975), Scots pine, *Pinus sylvestris* (Gu et al. 2001) as well as in our Douglas-fir specimen. Tracheid wall anisotropy could be important to directional aspects of dimensional stability and stiffness of wood (Gu et al. 2001; Murata and Masuda 2006). If so, a measure of anisotropy would be a useful feature to incorporate in SilviScan.

Wood density measurement by Ring Profiler is possible, but it suffers in the present implementation from inadequate image quality of latewood tracheids. The best way to improve image quality is by (1) adopting different methods of sample preparation (Reme and Helle 2002); and (2) using better illumination such as near-infrared through-the-side lighting or supplemental reflection lighting (Evans 1994).

ACKNOWLEDGMENT

We acknowledge Dr. Geoff Downes and his staff of the Commonwealth Scientific and Industrial Research Organization (Tasmania, Australia), who advised on SilviScan sample preparation and conducted SilviScan analysis.

REFERENCES

Cown, D. J. 1975. Variation in tracheid dimensions in the stem of a 26-year-old radiata pine tree. Appita 28(4): 237–245.

DeGroot, R. C., and T. A. Kuster. 1986. SEM X-Ray microanalysis of tracheid cell walls in southern yellow pine sapwood treated with water-dispersible pentachlorophenol. Wood Fiber Sci. 18(1):58–67.

Evans, R. 1994. Rapid measurement of the transverse dimensions of tracheids in radial wood sections from *Pinus radiata*. Holzforschung 48(2):168–172.

———, G. Downes, D. Menz, and S. Stringer. 1995. Rapid measurement of variation in tracheid transverse dimensions in a radiate pine tree. Appita J. 48(22):134–138.

———, R. P. Kibblewhite, and S. Stringer. 1997. Kraft pulp fiber property prediction from wood properties in eleven radiate pine clones. Appita J. 50(11):25–33.

———, ———, and M. Lausberg. 1999. Relationships between wood and pulp properties of twenty-five 13 year old radiate pine trees. Appita J. 52(22):132–139.

Gu, H., A. Zink-Sharp, and J. Sell. 2001. Hypothesis on the role of cell-wall structure in differential transverse shrinkage of wood. Holz Roh- Werkst. 59:436–442

Ivkovich, M., G. Namkoong, and M. Koshy. 2002. Genetic variation in wood properties of interior spruce. II Tracheid characteristics. Can J. For. Res. 32:2128–2139.

Jang, H. F., R. S. Seth, C. B. Wu, and B. K. Chan. 2005. Determining the transverse dimension of fibres in wood using confocal microscopy. Wood Fiber Sci. 37(4):615–628.

Jones, T. G., and S. R. Corson. 1996. Relationship of TMP and wood properties of radiata pine trees. Appita'96. p. 553.

Kang, K.-Y., S. Y. Zhang, and S. D. Mansfield. 2004. The effects of initial spacing on wood density, fibre and pulp properties in jack pine (*Pinus banksiana Lamb*.). Holzforschung 58(5):455–463.

Kellogg, R. M., and F. F. Wangaard. 1969. Variation in the cell-wall density of wood. Wood Fiber 1:180–204.

Kibblewhite, R. P., and A. D. Bawden. 1991. Fiber and fiber wall response to refining in softwood and hardwood pulps, preprint, Current and Future Technologies of Refining Conference. PIRA, Leatherhead, UK.

Klungness, J. H., R. Gleisner, D. Mann, K. Scallon, J. Y. Zhu, E. Horn, and L. L. Edwards. 2006. Evaluation of forest thinning materials for TMP production. TAPPI J. 5(4):17–22.

Liu, J., X. M. Diao, and T. Furuno. 2002. Quantitative analysis of morphological variation of cross sectional tracheids of Hinoki (*Chamaecyparis obtus* Endl.) near Knot by imaging processing. Holzforschung 56(3):239–243.

Midorikawa, Y., Y. Ishida, and M. Fujita. 2005. Transverse shape analysis of xylem ground tissues by Fourier transform image analysis I: Trial for statistical expression of cell arrangements with fluctuation. J. Wood Sci. 51: 201–208.

Murata, K. and M. Masuda. 2006. Microscopic observation of transverse swelling of latewood tracheid: Effect of macroscopic/mesoscopic structure. J. Wood Sci. 52:283–289.

Palviainen, J., and R. Silvennoinen. 2001. Inspection of wood density by spectrophotometry and a diffractive optical element based sensor. Meas. Sci. Technol. 12:345–352.

Reme, P. A., and T. Helle. 2002. Assessment of transverse dimension of wood tracheids using SEM and image analysis. Holz Roh- Werkst. 60:277–282.

Rudie, A. W., J. Morra, J. M. St. Laurent, and K. L. Kickey. 1994. The influence of wood and fiber properties on mechanical pulping. TAPPI J. 77(6):86–90.

Schimleck, L. R., and R. Evans. 2004. Estimation of *Pinus radiata* D. Don tracheid morphological characteristics by near infrared spectroscopy. Holzforschung 58:66–73.

———, P. D. Jones, G. F. Peter, R. F. Daniels, and A. Clark III. 2004. Nondestructive estimation of tracheid length from sections of radial wood strips by near infrared spectroscopy. Holzforschung 58:375–381.

Seth, R. S. 1990. Fibre quality factors in papermaking–II.

The importance of fibre coarseness. Pages 143–161 *in* Materials Research Society Symposium Proceedings, Vol. 197. Materials Research Society, Pittsburgh, PA.

———, H. F. JANG, B. K. CHAN, AND C. B. WU. 1997. Transverse dimensions of wood pulp fibers and their implications for end use. Pages 473–503 *in* The Fundamentals of Papermaking Materials; Transactions. 11th Fundamental Res. Symp. Cambridge, UK., C. F. Baker, ed., PIRA International, Leatherhead, UK.

SKINNARLAND, I., P. O. JOHNSEN, O. W. GREGERSEN, AND T. HELLE. 1995. Cross section characteristics of commercial papermaking pulp fibers, pages 91–93 *in* International Paper Physics Conference, Niagara-on-the-Lake, Ontario, CPPA (Tech. Sec.), Montreal, Canada.

ZHU, J. Y., D. W. VAHEY, T. C. SCOTT, AND G. C. MYERS. 2007. Effect of tree growth rate on papermaking fibre properties, *in* International Paper Physics Conference, Gold Coast, Australia. Pp. 415–422.